Published in final edited form as:
J Toxicol Environ Health A. 2010 ; 73(12): 819–836. doi:10.1080/15287391003689317.

Perfluorooctane sulfonate (PFOS) induces reactive oxygen species (ROS) production in human microvascular endothelial cells: role in endothelial permeability

Yong Qian[1,*], **Alan Ducatman**[2], **Rebecca Ward**[1], **Steve Leonard**[1], **Valerie Bukowski**[1], **Nancy Lan Guo**[2,3], **Xianglin Shi**[4], **Val Vallyathan**[1], and **Vincent Castranova**[1]

[1] Pathology and Physiology Research Branch, Health Effects Laboratory Division, National Institute for Occupational Safety and Health, Morgantown, WV 26505

[2] Department of Community Medicine, School of Medicine, West Virginia University, Morgantown, WV 26506-9190

[3] Mary Babb Randolph Cancer Center, School of Medicine, West Virginia University, Morgantown, WV 26506-9300

[4] Graduate Center for Toxicology, College of Medicine, University of Kentucky, Lexington, Kentucky 40536

Abstract

Perfluorooctane sulfonate (PFOS) is a member of perfluoroalkyl acids (PFAA) containing an 8-carbon backbone. PFOS is a man-made chemical with carbon-fluorine bonds that are one of the strongest in organic chemistry and widely used in industry. Human occupational and environmental exposure to PFOS occurs globally. PFOS is non-biodegradable and persistent in the human body and environment. In this study, data demonstrated that exposure of human microvascular endothelial cells (HMVEC) to PFOS induced the production of reactive oxygen species (ROS) at both high and low concentrations. Morphologically, it was found that exposure to PFOS induced actin filament remodeling and endothelial permeability changes in HMVEC. Furthermore, data demonstrated the production of ROS plays a regulatory role in PFOS-induced actin filament remodeling and the increase in endothelial permeability. Our results indicate that the generation of ROS may play a role in PFOS-induced aberrations of the endothelial permeability barrier. The results generated from this study may provide a new insight into the potential adverse effects of PFOS exposure on humans at the cellular level.

Keywords

Perfluorooctane sulfonate; PFOS; reactive oxygen species; permeability; actin filaments

Perfluoroalkyl acids (PFAA) are man-made chemicals with a carbon backbone 4–14 in length and a charged functional moiety (mainly carboxylate, sulfonate, or phosphonate) (Lau *et al*., 2007; Kovarova and Svobodova, 2008). The fluorine moiety of PFAA provides extremely low surface tension which renders PFAA a unique hydrophobic and oleophobic

[*]Corresponding author: Yong Qian, Pathology and Physiology Research Branch, Health Effects Laboratory Division, National Institute for Occupational Safety and Health, 1095 Willowdale Road, Morgantown, WV 26505-2888, Fax: (304) 285-5938, Tel: (304) 285-6286, yaq2@cdc.gov.

nature. Carbon-fluorine bonds within PFAA are among the strongest in organic chemistry. The fully fluorinated hydrocarbons are stable at temperatures as high as 150 °C and are nonflammable. PFAA are not subject to degradation by strong acids, alkalis, oxidizing agents, or photolysis (Lau *et al.*, 2007). These chemical and physical features point to a extremely stable character of PFAA, which makes these chemicals ideal surfactants in a variety of industries (Lau *et al.*, 2007). PFAA have a long history of industrial applications, and there is emerging appreciation of their potential biological activity (Lau *et al.*, 2007; Kovarova and Svobodova, 2008). PFAA are widely used as fluorocarbon-based industrial surfactants in aircraft production processes, automotive production processes, chemical products, building products, electronic products, and personal care products in the past half century. Until recently, PFAA have been considered biologically inactive (Andersen *et al.*, 2008). Nevertheless, their unique stability also makes these chemicals almost nonbiodegradable and persistent in the environment, which may pose a potential chronic health risk to humans (Lau *et al.*, 2007). The Center for Disease Control and Prevention (CDC) recently established biomonitoring for several members of PFAA in its National Health and Nutrition Examination Survey (NHANES) (Andersen *et al.*, 2008).

Although all PFAA share unique structural stability, the members with 8-carbon backbone are most effective and widely used in industry. Perfluorooctane sulfonate (PFOS) is a widely known PFAA containing an 8-carbon backbone (Kovarova and Svobodova, 2008). Human occupational and environmental exposure to PFOS occurs globally (Lau *et al.*, 2007). In 2000, world-wide industry produced and used 3,500 metric tons of PFOS (Lau *et al.*, 2007). Furthermore, PFOS is generated from the biodegradation of various precursors. Several studies demonstrated that there are more than 50 precursors of PFOS used in various industries (Pelley, 2004). Surveillance studies detected PFOS in biological samples from exposed individuals globally, and the concentrations of PFOS in wildlife as well as humans are greater than that of other members of PFAA (Kannan *et al.*, 2001; Taniyasu *et al.*, 2003). Under environmental conditions, PFOS shows high thermal, chemical, photolytic, and biological stability (Parsons *et al.*, 2008). Studies also demonstrated that PFOS is not metabolized in rats or humans (Olsen *et al.*, 2007). These unique features of PFOS indicate that PFOS has a potential to bioaccumulate. Indeed, the half-life for serum elimination of PFOS is approximately 88–146 days for male and female cynomolgus monkeys after initial intravenous dosing and repeated oral dosing (Seacat *et al.*, 2002; Olsen *et al.*, 2007). The half-life for serum elimination of PFOS among retired PFOS production workers is approximately 5.4 years (Kudo *et al.*, 2006; Olsen *et al.*, 2007).

PFOS enters the human body through ingestion and skin penetration (Kudo *et al.*, 2006), and binds proteins, such as serum albumin (Kovarova and Svobodova, 2008). Both in vivo and in vitro assays demonstrated that PFOS is highly bound in rat, monkey, and human plasma over a concentration range of 1–500 μg/ml (Olsen *et al.*, 2007). PFOS has a high affinity for β-lipoproteins and competes for fatty acid binding sites on liver fatty acid binding protein (Luebker *et al.*, 2002). PFOS binds DNA (Zhang *et al.*, 2009). Furthermore, it was demonstrated that the binding of PFOS to protein and DNA is via ion bonds, van der Waals force and hydrophobic interaction, which alter the secondary conformation of protein and DNA (Zhang *et al.*, 2009).

Several epidemiological and medical surveillance studies have been performed on general populations and occupational cohorts exposed to PFOS (Lau *et al.*, 2007; Olsen *et al.*, 2007). A cohort study of PFOS-exposed workers showed that bladder cancer mortality was elevated among male workers who had worked in a high volume PFOS exposure job for a minimum of one year; however, the results were only based on three cases (Alexander *et al.*, 2003). A recent Danish study found that high PFOS levels were associated with fewer normal sperm in young men (Joensen *et al.*, 2009). PFOS has also been associated with

decreased fecundity in women (Fei *et al.*, 2009). Due to the placental transfer of PFOS in humans, epidemiologic studies also focused on the effects of PFOS exposure on human fetal development. Recent studies showed conflicting conclusions regarding maternal exposures to low levels of PFOS and newborn birth weight (Hamm *et al.*, 2009; Washino *et al.*, 2009). An epidemiologic assessment of 5,262 pregnancies in mid-Ohio Valley residents (2000–2006) reported modest associations of PFOS exposure with preeclampsia and low birth weight (adjusted odds ratio = 1.3, 95% confidence interval: 1.1, 1.7) (Stein *et al.*, 2009). Significant associations between PFOS exposure and high serum cholesterol have been reported (Steenland *et al.*, 2009). Preliminary data suggest possible interactions with thyroid homeostasis, but outcomes are not consistent in all studies (Olsen *et al.*, 2003a; Bloom *et al.*, 2009; Dallaire *et al.*, 2009).

PFOS-induced adverse effects from animal studies include body weight reduction, hepatomegaly and hepatic peroxisome proliferation, hormone disruption, immunotoxicity, and neonatal mortality (Lau *et al.*, 2007). The molecular mechanism underlying PFOS-induced harmful effects on animals is not yet fully elucidated. Currently, Lau et al (2007) and DeWitt et al (2009) found that the activation of peroxisome proliferator-activated receptor-alpha (PPAR-α) signaling pathway may play a major role. Gene expression profiling in the liver and lung of PFOS-exposed mouse fetuses confirmed that PFOS-dependent changes are primarily related to activation of PPAR-α (Rosen *et al.*, 2009). However, increasing evidence from other animal studies also demonstrated that PFOS-induced toxicity can be independent of PPAR-α activation (Lau *et al.*, 2007; Abbott *et al.*, 2009; DeWitt *et al.*, 2009).

It was found that exposure to high concentrations of PFOS induced lipid peroxidation in rat neuronal PC12 cells lines, which directly resulted in developmental neurotoxicity (Slotkin *et al.*, 2008). Short-term exposures of fish to high concentrations of PFOS consistently increased hepatic fatty acyl-CoA oxidase activity and oxidative damage (Oakes *et al.*, 2005). Recently, a study found that PFOS exposure induced the production of reactive oxygen species (ROS) in human hepatoma Hep G2 cells (Hu and Hu, 2009). The present study investigated whether PFOS exposure would induce ROS production in human microvascular endothelial cells (HMVEC) as well as mouse macrophages. Furthermore, the time course and the dose-dependence of PFOS-induced ROS production were evaluated. The present study also attempted to determine whether exposure to PFOS induces permeability changes in HMVEC. Moreover, the role of ROS production in PFOS-induced permeability in HMVEC was evaluated.

Materials and Methods

Materials

Perfluorooctane sulfonate (PFOS) and catalase were purchased from Sigma-Aldrich (St. Louis, MO). Cell culture media EBM-2 was obtained from Lonza (Boston, MA). Fetal bovine serum was obtained from Atlanta Biologicals (Lawrenceville, GA). Penicillin and streptomycin, 5-(and-6)-chloromethyl-2′,7′-dichlorodihydrofluorescein diacetate, acetyl ester (CM-H_2DCFDA), FITC-phalloidin, dihydroethidium (DHE), secondary antibodies-conjugated with FITC, TRITC, and Cy5 were purchased from Invitrogen (Eugene, OR). VE-Cadherin antibody was purchased from Alexis (San Diego, CA). Electrical cell substrate impedance sensing system (ECIS) culture wares were purchased from Applied Biophysics (Troy, NY). PFOS stock solution (1M) was prepared in 1×PBS with 10% DMSO, and was then diluted to 1 mM PFOS working solution with serum free cell culture medium.

Cell culture

Mouse Raw 264.7 macrophages purchased from ATCC (Manassas, VA) were cultured according to the protocol provided by ATCC. The human microvascular endothelial cells (HMVEC) were a kind gift from Dr. Rong Shao (Biomedical Research Institute, Baystate Medical Center/University of Massachusetts at Amherst, Springfield, MA, USA). HMVEC were cultured according to the protocol described previously (Shao and Guo, 2004). Briefly, HMVEC were grown in endothelial basal medium-2 (EBM-2) (Lonza, Boston MA) supplemented with 10% (v/v) fetal bovine serum (FBS) (Atlanta Biologicals, Lawrenceville, GA), 100 U/ml penicillin,10 μg/ml streptomycin, 0.01μg/ml of epidermal growth factor and 1μg/ml hydrocortisone. The cells were maintained in an incubator at 37 °C with 5% CO_2 in air.

Electron Spin Resonance (ESR) Spectroscopy

Since free radicals are reactive and have short life-time, direct ESR measurements can not be used for their detection. Instead, ESR spin trapping, an indirect method, was used to detect short-lived free radicals such as hydroxyl (˙OH). This method is based on there action of a short-lived radical binding with a paramagnetic compound to form a relatively long-lived free radical product(spin adduct). This adduct can then be observed using conventional ESR whereby the intensity of the signal is used to measure the amount of short-lived radicals trapped. The hyperfine couplings of the spin adduct are generally characteristics of the original trapped radicals. This method is ideal for detection and identification of free radicals because of its specificity and sensitivity. All ESR measurements were conducted using a Bruker EMX spectrometer (Bruker Instruments Inc., Billerica, MA 01821, USA) and a flat cell assembly. Hyperfine couplings were measured (to 0.1 G) directly from magnetic field separation using potassium tetraperoxochromate (K_3CrO_8) and 1,1-diphenyl-2-picrylhydrazyl (DPPH) as reference standards(Buettner, 1987; Janzen *et al.*, 1987). The Acquisit program was used for data acquisitions and analyses (Bruker Instruments Inc., Billerica, MA 01821, USA). RAW 264.7 macrophages (1×10^6/ml) were suspended in 1× PBS pH 7.4 and incubated with the spin trap 5,5-dimethyl-1-pyrroline-N-oxide (DMPO; 200mM) in the presence or absence of different concentrations of PFOS. Samples were incubated for 5 min in a 37° C water bath and than transferred to an ESR flat cell for measurement at room temperature with instrument settings of 63.6 milliwatt, modulation amplitude 1G, receiver gain 1.00×10^4, conversion time 40.960 msec, and time constant 40.960 msec. All Spectra shown are in accumulation of 5 scans. The relative radical concentration was estimated by measuring the peak-to-peak height (mm) of the observed spectra.

Transendothelial electrical resistance

The transendothelial electrical resistance (TER) was measured using electrical cell—substrate impedance sensing system (ECIS) (Applied Biophysics, Troy, NY) according to the published protocol (Babior, 2000; Apopa *et al.*, 2009). Measuring transendothelial electrical resistance is a measure of endothelial barrier integrity. Briefly, HMVEC were grown to confluent monolayers on ECIS culture ware and serum-starved overnight. The electrical resistance was measured on cells located on the small gold electrodes in each of the wells. The culture medium was the electrolyte. The small gold electrode covered by confluent HMVEC and a larger gold counter electrode were connected to a phase-sensitive lock-in amplifier. A constant current of 1 μA was supplied by a 1 V, 4,000 Hz alternating current through a 1 M resistor. Changes in voltage between the small electrode and the large counter electrode were continuously monitored by the lock-in amplifier, stored, and then calculated as resistance.

Immunofluorescence confocal microscopy assay

Immunofluorescence assays were performed according to the methods published previously (Qian *et al.*, 2005). Briefly, HMVEC were grown oncoverslides. After treatment, cells were fixed and permeabilized, followed by labeling with the specific antibodies for the targeted proteins as well as immunofluorescence-conjugated secondary antibodies. The labeled coverslides were mounted to the slides with an antifade reagent (Invitrogen, Eugene, OR). A Zeiss LSM 510 microscope was used to obtainimages. Scale bars were generated and inserted by LSM software.

ROS measurement by confocal microscopy

ROS measurements by confocal microscopy were performed according to the methods described previously (Qian *et al.*, 2003b and 2005). Briefly, confluent HMVEC were serum-starved overnight and then stimulated with different concentrations of PFOS for varying time periods. During the simulation periods, dihydroethidium (DHE) was added at a final concentration of 5 μM for the last 30 min of exposure. After incubation, the cells were washed twice with phosphate-buffered saline and mounted on coverslips. A Zeiss LSM 510 microscope was used to obtain images. Scale bars were generated and inserted by LSM software.

ROS measurement by a fluorescence microplate reader

HMVEC were plated at 2×10^5 in 24 well plates grown to confluence, and serum-starved overnight. The cells were first measured at the appropriate wavelengths using a CytoFluor plate reader to determine the cellular background. The cells were then treated with PFOS. One hr prior to reading the fluorescence of the samples, 5μM DHE was added. Fluorescence was immediately measured for background (excitation = 485/20, emission = 580/20, gain = 50), and then measured at one-hr increments for the duration of the experiment. The background fluorescence of the cells and cells with the dye were then subtracted from values of fluorescence for each treatment. The untreated samples were set to 1 by division, and the treated samples scaled appropriately.

Statistics

One-way ANOVA test was used to determine statistical significance for ROS measurement by a fluorescence microplate reader. A student's paired *t* test was appled to determine statistical significance for ROS measurement by ESR spectroscopy. The criteria for significance was set at $p<0.05$.

Results

PFOS induces ROS generation in macrophages

The ESR technique was applied for radical detection due to its specificity for free radical measurements. Since ESR studies must be performed without the presence of media or fetal bovine serum, the reactions can only be measured for short time periods up to about 30 min. These unique requirements of ESR measurements suggest that both high concentrations of PFOS and a robust cell system are needed to observe the production of ROS. Macrophages were selected in the ESR analysis due to their highly reactive activities within short period of exposure time in PBS (Leonard *et al.*, 2004 and 2007).

High range concentrations of PFOS were selected to expose macrophages according to published results (Oakes *et al.*, 2005; Slotkin *et al.*, 2008; Hu and Hu, 2009). In Figure 1B, the two center peaks were measured and averaged for a sample n=4. Hydroxyl radical gives a 1:2:2:1 pattern with a splitting constant of 14.9 gauss. Both the pattern and the splitting

constants helped define the peak. However further use of the scavengers catalase and superoxide dismutase verified the identity as superoxide radical and hydroxyl radical. The peaks in Figure 1B might not be strong; however, they were consistent over the 4 replicates. Moreover, there were no peaks without PFOS (Figure 1A). Taken together, the results demonstrate that PFOS increased ROS generation by 3.4 fold in macrophages (Figure 1C).

Exposure to high range concentrations of PFOS induces ROS generation in HMVEC

PFOS-induced ROS production in HMVEC was examined using confocal microscopy analysis. HMVEC were exposed to different concentrations (10–100 μM) of PFOS for one hr, followed by incubation with dihydroethidium for the last 30 min of exposure. Dihydroethidium is a dye that stains cells blue. When it is degraded by $O_2^{\cdot -}$, the blue color decreases and the degradation products stain cells red. The measurements of intensity of two different colors reflect the amounts of ROS production in cells in an opposite way (i.e., the intensity of red color directly correlates with the ROS production in cells while the blue staining inversely correlates with the ROS production). The untreated cells showed a weak red staining while the PFOS treated cells exhibited a strong red staining, which increases with PFOS exposure from 10–100 μM (Figure 2A). Results demonstrate that exposure of HMVEC to PFOS induced the production of ROS over a concentration range of 10–100 μM.

Fluorescence-based microplate reader analysis was performed to quantify PFOS-induced ROS production in HMVEC. HMVEC were exposed to two different concentrations of PFOS at 50 μM and 100 μM for 1 hr, followed by incubation with dihydroethidium for the last 30 min of exposure. The results show that PFOS exposure induced a significant increase (2 fold) of ROS generation at the concentrations of 50–100 μM in HMVEC (Figure 2B).

Exposure to low range concentrations of PFOS induces the production of ROS in HMVEC

Since serum PFOS levels in occupational workers are typically between 0.5–2 μg/ml (about 1–5 μM), with the highest level reaching 13 μg/ml (26 μM) (Olsen *et al.*, 1998; Olsen *et al.*, 2003a; Olsen *et al.*, 2003b; Lau *et al.*, 2007; Slotkin *et al.*, 2008), it is relevant to explore PFOS-induced ROS production at the concentrations within these occupational exposure ranges in the cellular test system. HMVEC were exposed to PFOS at the low range concentrations (2 or 5 μM) for 1 hr as indicated, followed by the incubation with dihydroethidium for the last 30 min of exposure (Figure 3A). The untreated cells exhibited strong blue staining, whereas 2 μM PFOS exposure substantially decreased the intensity of blue staining and 5 μM PFOS exposure almost eliminated the blue staining. The results demonstrate that PFOS induced ROS production over low range concentrations between 2–5 μM within 1 hr (Figure 3A). The results also indicate that PFOS may induce ROS production in a concentration-dependent manner in HMVEC.

The time course of PFOS-induced ROS production in HMVEC was also evaluated. Results indicate that PFOS-induced production of ROS in HMVEC increased with increasing of incubation time (over 1–5 hrs) at the concentration of 2 μM (Figure 3B).

PFOS induces permeability in HMVEC through production of ROS

The vascular endothelial monolayer forms a semi-selective permeability barrier between blood and the interstitial space to control the movement of blood fluid, proteins, and macromolecules across the vessel wall (Mehta and Malik, 2006). Morphologically, the increase in endothelial cell permeability mainly results from disruption of cell junctions and cell adhesions, which leads to the formation of gaps between endothelial cells (Mehta and Malik, 2006). Whether PFOS exposure could induce permeability changes in HMVEC monolayers was determined by measuring transendothelial electrical resistance.

The confluent monolayer of HMVEC was exposed to PFOS at different concentrations (2 or 5 μM) as indicated in Figure 4A. During the exposures, an electric cell-substrate impedance sensor (ECIS) was used to measure transendothelial electrical resistance (TER), which reflects the permeability of HMVEC monolayer. The change in TER reading inversely correlates with an increase in permeability. The results show that exposure of HMVEC to PFOS induced a decrease in resistance, which correlates with an increase in permeability in HMVEC, at PFOS concentrations as low as 2 μM (Figure 4A). Furthermore, exposure to 5 μM of PFOS decreased resistance to a greater extent than 2 μM, suggesting that PFOS induces endothelial permeability in a concentration-dependent manner. Thus, results demonstrate that PFOS exposure may compromise the integrity of the endothelial monolayer barrier.

To visualize the effect of PFOS-induced endothelial monolayer barrier change, confocal microscopy imaging analysis technique was employed to image the cell junctions of the monolayers with fluorescence-conjugated specific antibodies to cell membrane protein VE-cadherin. The results show that HMVEC in the untreated monolayers align tightly with no significant gaps detected between cells. However, upon exposure to 2 μM of PFOS, many gaps were apparent in the HMVEC monolayers. Furthermore, it was found that 5 μM of PFOS induced more gap formation than 2 μM (Figure 4B). These results again suggest that PFOS exposure induced an increase in permeability in a concentration-dependent manner in HMVEC monolayers.

It was proposed that ROS might increase endothelial permeability (Lum and Roebuck, 2001; Houle and Huot, 2006). Therefore, experiments were conducted to determine whether the PFOS-induced permeability increase is modulated through ROS production in HMVEC. A specific ROS scavenger, catalase (2,000 units/ml), was added into HMVEC monolayers, followed by PFOS stimulation and confocal microscopy imaging analysis. Results demonstrate that inhibition of ROS production substantially blocked the PFOS-induced gap formation in HMVEC, indicating that the production of ROS may play a regulatory role in the PFOS-induced permeability increase in HMVEC (Figure 4C).

PFOS induces actin filament remodeling through the production of ROS in HMVEC

In endothelial cells, actin filaments are key components of cell junctions and adhesions and are involved in modulating endothelial permeability (Mehta and Malik, 2006). The remodeling of actin filaments induces the formation of central stress fibers to develop strong substrate anchorage, and peripheral motile structures of lamellipodia and filopodia for cell spreading and motility (Lee and Gotlieb, 2002). The change in endothelial permeability is directly associated with actin filament remodeling (Mehta and Malik, 2006).

FITC-phalloidin was used to stain actin filaments in HMVEC, followed by confocal microscopy imaging analysis. Results demonstrate that HMVEC in the unstimulated monolayers closely attach each other to form a well-organized network structure and are separated by an evenly distributed actin dense periphery band (DPB). However, upon PFOS exposure for one hr, both the network structure and the DPB were disrupted, the cells pulled apart, and some small breaks were formed in the monolayers (Figure 5A). The results demonstrate that PFOS exposure induced actin filament remodeling in monolayer HMVEC. To explore the regulatory role of ROS in PFOS-induced actin filament remodeling, the HMVEC monolayer was pretreated with catalase to remove ROS, followed by 2 μM of PFOS exposure and confocal microscopy imaging analysis. Results indicate that the removal of ROS substantially blocked PFOS-induced actin filament remodeling, indicating the regulatory role of ROS in PFOS-induced actin filament remodeling in HMVEC (Figure 5B).

Since it is difficult to measure actin filament remodeling at the cell peripheral region in a closely attached HMVEC monolayer, subconfluent HMVEC were exposed to 2 μM of PFOS for 1 hr to determine whether the exposure would induce actin filament remodeling at the peripheral region to form cell motile structures, such as lamellipodia and filopodia. Results demonstrate that PFOS exposure induced actin filament remodeling to form lamellipodia and filopodia structures at the cell periphery and stress fiber structures in the cell body, and that inhibition of ROS production by catalase blocked PFOS-induced formation of lamellipodia, filopodia, and stress fibers (Figure 5C). These results demonstrate that PFOS exposure has an ability to remodel actin filaments through the ROS production.

Discussion

According to the preliminary data from West Virginia University, consistent statistically significant associations of serum electrolytes with PFAA serum values in a large survey population have been noted (preliminary data available at http://www.hsc.wvu.edu/som/cmed/c8/). This might result from PFAA-induced vascular endothelium barrier dysfunction. A 30 year medical surveillance has also found an association between elevated uric acid levels and perfluorooctanoic acid (PFOA), another key member of PFAA, concentrations in human serum (Costa *et al.*, 2009). Hyperuricemia was found to induce endothelial dysfunction (Nakagawa *et al.*, 2006). Moreover, it was suggested that dysfunction of vascular system may be associated with low birth weight (Holt and Byrne, 2002; Norman, 2008). A single human study with unconventional study design raised an association between PFAA exposures and human cardiovascular disease (Anderson-Mahoney *et al.*, 2008). This study has several limitations, and the question of human cardiovascular disease awaits its first large-scale population evaluation with incident-epidemiologic designs. More fundamentally, PFOS does induce oxidative stress and is known to change surface membrane potential and to alter calcium channels (Harada *et al.*, 2005). Furthermore, glucose homeostasis and hepatic metabolism appear to be systemically affected, in studies using NHANES data (Lin *et al.*, 2009a and 2009b). There is ample physiologic reason to consider endothelial response in cell system and toxicity studies, as well as cardiovascular disease in future incident studies of human populations. Therefore, it is postulated that the identification of PFOS-induced endothelial dysfunction may provide some fundamental information concerning adverse health effects on humans.

In this report, human microvascular endothelial cells (HMVEC), an *in vitro* human microvascular endothelium model, were used. This model was generated through immortalization of primary endothelial cells by engineering with a human telomerase catalytic protein (hTERT) (Shao and Guo, 2004). This cell model resembles the signature of primary human microvascular endothelial cells in phenotype and gene expression profile more than a commercially available human microvascular endothelial cell-1 (HMEC-1) cell line does. HMEC-1 were established by the transduction of SV40 large T antigen. The availability of this model in our laboratory provides us with a unique advantage in the study of PFOA and PFOS-induced effects on endothelium. We have applied this model to successfully identify the toxic effects of iron oxide nanoparticles *in vitro (*Apopa et al., 2009).

The results of this study demonstrate that exposure of HMVEC to both high and low concentrations of PFOS induced the production of ROS. Morphologically, PFOS exposure induced actin filament remodeling and endothelial permeability changes in HMVEC. Furthermore, the production of ROS appeared to play a regulatory role in PFOS-induced actin filament remodeling and endothelial permeability increase. Taken together, the results lead us to hypothesize that PFOS-induced ROS production plays a role in the aberrations of the endothelial permeability barrier. Aberrations of endothelial permeability were reported

to play a major role in the pathogenesis of many human diseases, including inflammation, acute lung injury syndromes, and carcinogenesis (Houle and Huot, 2006; Mehta and Malik, 2006). Therefore, results from the present study provide insight into potential mechanisms for the effects of PFOS exposure upon humans at the cellular level.

Reactive oxygen species (ROS) refer to a diverse group of reactive, short-lived, oxygen containing species, such as $O_2^{\cdot -}$, H_2O_2, and $^{\cdot}OH$. Cellular systems are protected from ROS-induced cell injury by an array of defenses composed of various antioxidants with different functions. When ROS in the cellular system overpower the defense systems, ROS produce cell damage or oxidative stress, leading to the development of various diseases. ROS possess five crucial properties of cell injury with capacities: (a) to cause permanent structural changes in DNA, (b) to initiate lipid peroxidation, (c) to induce protein oxidation, (d) to modulate the activity of stress proteins and stress genes that regulate effector genes related to growth, differentiation, and cell death, and (e) to activate cytoplasmic and nuclear signal transduction pathways (Qian *et al.*, 2003a). ROS have been implicated to be involved in many diseases, ranging from cardiovascular disorders, carcinogenesis, chronic inflammation, and neurodegenerative diseases (Halliwell *et al.*, 1992; Gutteridge and Halliwell, 2000). Two separate studies from other research groups suggested that PFOS-induced oxidative stress response was involved in developmental neurotoxicity in PC12 cells, a neuronotypic cell line (Slotkin *et al.*, 2008), and hepatic fatty acyl-CoA oxidase activity increase in fish (Oakes *et al.*, 2005). Recently, a report showed that exposure of human hepatoma HepG2 cells to 50–200 μM PFOS induced ROS production, leading to dissipation of mitochondria membrane potential and induction of apoptosis (Hu and Hu, 2009).

Wei and colleagues (2009) found that PFOA and PFOS mixtures affect minnow genes implicated in oxidative stress. Huang and colleagues (2009) used PFOS to induce oxidative stress in Atlantic salmon. Nakayama and colleagues (2008) report that PFOS concentration is positively correlated with mRNA levels of glutathione peroxidase 1 and glutathione-s-transferase alpha 3 in cormorant liver, as well as negatively correlated with the response of heat shock protein 8. They inferred that antioxidant enzymes are induced in response to oxidative stress and suppression of molecular chaperones, from PFC exposure, leading to reductions in protein stability (Nakayama *et al.*, 2008). In human population studies, the consistent and strong association of biomarkers of PFOS with elevated lipids suggests a further reason to examine oxidative stress in humans, especially since humans do not metabolize or excrete longer-chain perfluorocarbons readily (Steenland *et al.*, 2009; Nelson, *et al*., 2010).

However, a potentially important issue raised from these results is that the concentrations of PFOS applied in these assays were substantially higher than the concentrations relevant to occupational and environmental exposures. Serum PFOS levels in occupational workers are typically between 0.5–2 μg/ml (about 1–5 μM), with the highest level reaching 13 μg/ml (26 μM) (Olsen *et al.*, 1998; Lau *et al.*, 2007; Slotkin *et al.*, 2008). In the general population, serum PFOS levels were reported to be approximately 20 ng/ml (40 nM) (Calafat *et al.*, 2007 and 2007b; Slotkin *et al.*, 2008). Therefore, one could argue that identification of PFOS-induced ROS at the low range concentrations may yield more relevant data. In the present study, both macrophages and HMVEC were initially exposed to high-range concentrations of PFOS to determine their capability to produce ROS according to previously published dose ranges (Oakes *et al.*, 2005; Slotkin *et al.*, 2008; Hu and Hu, 2009). Then, HMVEC were exposed to occupationally and environmentally relevant low concentrations of PFOS to detect its capability to produce ROS and HMVEC effects. Results demonstrate that PFOS exposure was able to induce ROS production in an in vitro human endothelial cell system within the occupationally and environmentally exposure-

relevant concentration ranges, which implies that human exposure to PFOS at ranges compatible with biomonitoring results might induce the generation of ROS.

In this study, three different techniques were used to measure PFOS-induced ROS production in both macrophages and HMVEC to take advantage of the unique features of each individual technique. To evaluate the production of PFOS-induced ROS in macrophages, ESR spin trapping was used. Spin trapping is the method of choice for detection and identification of free radical generation in biological systems due to its specificity and sensitivity (Qian *et al.*, 2001). Confocal microscopy imaging analysis was also used to examine PFOS-induced ROS in HMVEC. In recent years, the molecular staining techniques have been significantly improved to serve as additional methods to identify and characterize specific ROS. The confocal microscopy imagining analysis technique provides the physical images of ROS production in the cell system, as well as information about whether the free radicals are produced intracellularly or extracellularly. To further quantify the production of ROS, a fluorescence microplate reader was used to measure PFOS-induced ROS production in HMVEC. With these three different techniques, results indicate that PFOS exposure induced significant amounts of superoxide radical and hydroxyl radical production intracellularly in both human endothelial cells and mouse macrophages.

Colorimetric changes reflect the production of ROS in HMVEC (Figures 2 and 3). In Figure 2, reflecting a concentration range of PFOS between 0 to100 μM, the difference of ROS production was large and the change in red color staining substantial, which was easily detected by a confocal microscope. In contrast, in Figure 3, the concentration range of PFOS was between 0 to 5 μM, and the difference of ROS production was small. The change in red color staining was not detected by a confocal microscope. However, the changes in the blue color staining, which measure how much the dye was degraded by ROS, were substantial (Figure 3), indirectly reflecting the amount of PFOS-induced ROS production in HMVEC.

The results of this study indicate that PFOS exposure induced an alteration in endothelial permeability. Mechanistically, data show that PFOS-induced endothelial permeability was modulated by production of ROS. These results regarding the role of ROS in endothelial cell permeability are consistent with several published observations by other researchers that ROS-induced oxidant stress directly increases endothelial permeability (Lum and Roebuck, 2001; Houle and Huot, 2006). It was found that exposure of endothelial cell monolayer to ROS generators, xanthine/xanthine oxidase or glucose/glucose oxidase, increased endothelial cell permeability in a concentration-dependent manner (Shasby *et al.*, 1985; Holman and Maier, 1990). Furthermore, the direct stimulation of endothelial cells with H_2O_2 induced an increase in monolayer permeability (Siflinger-Birnboim *et al.*, 1996). Our published results showed that ROS production mediates iron oxide nanoparticle-induced permeability in HMVEC (Apopa *et al.*, 2009).

In this study, it was also found that PFOS-induced endothelial permeability may be associated with remodeling of actin filaments. Actin is one of the most abundant proteins in eukaryotic cells. There are two different forms of actin, monomeric actin (G-actin) and actin filaments (F-actin). Actin filaments are involved in a wide variety of cellular processes, including cell permeability, cell motility, cell cycle control, cellular structure, and cell signaling (Schmidt and Hall, 1998). They function in cellular processes by undergoing a dynamic structural remodeling as well as continuing polymerization and depolymerization, leading to the formation of discrete structures at the cell periphery for attachment to the substratum in response to extracellular signal transduction (Qian *et al.*, 2002). Compelling evidence showed that actin filament remodeling plays a major role in determining the structural integrity of the confluent endothelial monolayer (Lee and Gotlieb, 2003). In

endothelial cells, actin filaments are the key components of cell junctions and adhesions. Actin filaments undergo dynamic remodeling to form DPB in maintaining cell-cell adhesion, central stress fibers to develop strong substrate anchorage, and lamellipodia and filopodia for cell spreading and motility (Lee and Gotlieb, 2002). Mehta and Malik (2006) demonstrated that the disruption of actin filaments is directly related to an increase in endothelial cell permeability. Studies also found that both the reduction of DPB and the induction of stress fibers are associated with agonist-induced cell permeability changes (Vyalov *et al.*, 1996). The results from Figure 5 demonstrate that exposure of HMVEC to PFOS disrupted the integrity of DPB and induced the formation of lamellipodia, filopodia and stress fibers, which may generate the force to pull monolayer HMVEC apart. The results also demonstrate that the removal of ROS by catalase abolished PFOS-induced actin filament remodeling and HMVEC monolayer separation, resulting in an inhibition of PFOS-induced increase of endothelial permeability. Furthermore, PFOS-induced actin filament remodeling was concurrent with PFOS-induced endothelial cell permeability. Therefore, our results suggest that PFOS increases endothelial monolayer permeability through the production of ROS, which may in turn stimulate remodeling of actin filaments. This scheme is summarized in Figure 6.

In the current study, dihydroethidium dye was used to determine the PFOS-induced production of ROS in HMVEC. Future studies are needed to examine a) the source of ROS production and b) the mechanism by which ROS produce actin filament remodeling and endothelial cell permeability.

Acknowledgments

Dr. Nancy Lan Guo was supported by two grants from NIH (NIH R01LM009500 and NCRR P20RR16440). Dr. Ducatman's efforts are partially supported by the Mitchell M. Benedict and Helen L. Benedict Endowment Fund, as well as by a contract from Brookmar, Inc., who performed medical surveillance for PFOA settlement-class participants in the mid-Ohio Valley.

References

Abbott BD, Wolf CJ, Das KP, Zehr RD, Schmid JE, Lindstrom AB, Strynar MJ, Lau C. Developmental toxicity of perfluorooctane sulfonate (PFOS) is not dependent on expression of peroxisome proliferator activated receptor-alpha (PPAR alpha) in the mouse. Reprod Toxicol. 2009; 27:258–265. [PubMed: 18595657]

Alexander BH, Olsen GW, Burris JM, Mandel JH, Mandel JS. Mortality of employees of a perfluorooctanesulphonyl fluoride manufacturing facility. Occup Environ Med. 2003; 60:722–729. [PubMed: 14504359]

Andersen ME, Butenhoff JL, Chang SC, Farrar DG, Kennedy GL Jr, Lau C, Olsen GW, Seed J, Wallace KB. Perfluoroalkyl acids and related chemistries--toxicokinetics and modes of action. Toxicol Sci. 2008; 102:3–14. [PubMed: 18003598]

Anderson-Mahoney P, Kotlerman J, Takhar H, Gray D, Dahlgren J. Self-reported health effects among community residents exposed to perfluorooctanoate. New Solut. 2008; 18:129–143. [PubMed: 18511391]

Apopa PL, Qian Y, Shao R, Guo NL, Schwegler-Berry D, Pacurari M, Porter D, Shi X, Vallyathan V, Castranova V, Flynn DC. Iron oxide nanoparticles induce human microvascular endothelial cell permeability through reactive oxygen species production and microtubule remodeling. Part Fibre Toxicol. 2009; 6:1. [PubMed: 19134195]

Babior BM. The NADPH oxidase of endothelial cells. IUBMB Life. 2000; 50:267–269. [PubMed: 11327320]

Bloom MS, Kannan K, Spliethoff HM, Tao L, Aldous KM, Vena JE. Exploratory assessment of perfluorinated compounds and human thyroid function. Physiol Behav. 2009 [Epub ahead of print].

Buettner GR. Spin trapping: ESR parameters of spin adducts. Free Radic Biol Med. 1987; 3:259–303. [PubMed: 2826304]

Calafat AM, Kuklenyik Z, Reidy JA, Caudill SP, Tully JS, Needham LL. Serum concentrations of 11 polyfluoroalkyl compounds in the u.s. population: data from the national health and nutrition examination survey (NHANES). Environ Sci Technol. 2007a; 41:2237–2242. [PubMed: 17438769]

Calafat AM, Wong LY, Kuklenyik Z, Reidy JA, Needham LL. Polyfluoroalkyl chemicals in the U.S. population: data from the National Health and Nutrition Examination Survey (NHANES) 2003–2004 and comparisons with NHANES 1999–2000. Environ Health Persp. 2007b; 115:1596–1602.

Costa G, Sartori S, Consonni D. Thirty years of medical surveillance in perfluorooctanoic acid production workers. J Occup Environ Med. 2009; 51:364–372. [PubMed: 19225424]

Dallaire R, Dewailly E, Pereg D, Dery S, Ayotte P. Thyroid function and plasma concentrations of polyhalogenated compounds in Inuit adults. Environ Health Persp. 2009; 117:1380–1386.

DeWitt JC, Shnyra A, Badr MZ, Loveless SE, Hoban D, Frame SR, Cunard R, Anderson SE, Meade BJ, Peden-Adams MM, Luebke RW, Luster MI. Immunotoxicity of perfluorooctanoic acid and perfluorooctane sulfonate and the role of peroxisome proliferator-activated receptor alpha. Crit Rev Toxicol. 2009; 39:76–94. [PubMed: 18802816]

Fei C, McLaughlin JK, Lipworth L, Olsen J. Maternal levels of perfluorinated chemicals and subfecundity. Human Reprod. 2009; 24:1200–1205.

Gutteridge JM, Halliwell B. Free radicals and antioxidants in the year 2000. A historical look to the future. Ann N Y Acad Sci. 2000; 899:136–147. [PubMed: 10863535]

Halliwell B, Gutteridge JM, Cross CE. Free radicals, antioxidants, and human disease: where are we now? J Lab Clin Med. 1992; 119:598–620. [PubMed: 1593209]

Hamm MP, Cherry NM, Chan E, Martin JW, Burstyn I. Maternal exposure to perfluorinated acids and fetal growth. J Expo Sci Environ Epidemiol. 2009 [Epub ahead of print].

Harada K, Xu F, Ono K, Iijima T, Koizumi A. Effects of PFOS and PFOA on L-type Ca2+ currents in guinea-pig ventricular myocytes. Biochem Biophys Res Commun. 2005; 329:487–494. [PubMed: 15737613]

Holman RG, Maier RV. Oxidant-induced endothelial leak correlates with decreased cellular energy levels. Am Rev Respir Dis. 1990; 141:134–140. [PubMed: 2297171]

Holt RI, Byrne CD. Intrauterine growth, the vascular system, and the metabolic syndrome. Semin Vasc Med. 2002; 2:33–43. [PubMed: 16222594]

Houle F, Huot J. Dysregulation of the endothelial cellular response to oxidative stress in cancer. Mol Carcinogen. 2006; 45:362–367.

Hu XZ, Hu DC. Effects of perfluorooctanoate and perfluorooctane sulfonate exposure on hepatoma Hep G2 cells. Arch Toxicol. 2009; 83:851–861. [PubMed: 19468714]

Huang TS, Olsvik PA, Krovel A, Tung HS, Torstensen BE. Stress-induced expression of protein disulfide isomerase associated 3 (PDIA3) in Atlantic salmon (Salmo salar L.). Comp Biochem Physiol B Biochem Mol Biol. 2009; 154:435–442. [PubMed: 19747560]

Janzen EG, Towner RA, Haire DL. Detection of free radicals generated from the in vitro metabolism of carbon tetrachloride using improved ESR spin trapping techniques. Free Radic Res Commun. 1987; 3:357–364. [PubMed: 2854531]

Joensen UN, Bossi R, Leffers H, Jensen AA, Skakkebaek NE, Jorgensen N. Do perfluoroalkyl compounds impair human semen quality? Environ Health Persp. 2009; 117:923–927.

Kannan K, Koistinen J, Beckmen K, Evans T, Gorzelany JF, Hansen KJ, Jones PD, Helle E, Nyman M, Giesy JP. Accumulation of perfluorooctane sulfonate in marine mammals. Environ Sci Technol. 2001; 35:1593–1598. [PubMed: 11329707]

Kovarova J, Svobodova Z. Perfluorinated compounds: occurrence and risk profile. REVIEW. Neuro Endocrinol Lett. 2008; 29:599–608. [PubMed: 18987583]

Kudo N, Suzuki-Nakajima E, Mitsumoto A, Kawashima Y. Responses of the liver to perfluorinated fatty acids with different carbon chain length in male and female mice:in relation to induction of hepatomegaly, peroxisomal beta-oxidation and microsomal 1-acylglycerophosphocholine acyltransferase. Biol Pharm Bull. 2006; 29:1952–1957. [PubMed: 16946516]

Lau C, Anitole K, Hodes C, Lai D, Pfahles-Hutchens A, Seed J. Perfluoroalkyl acids: a review of monitoring and toxicological findings. Toxicol Sci. 2007; 99:366–394. [PubMed: 17519394]

Lee JS, Gotlieb AI. Microtubule-actin interactions may regulate endothelial integrity and repair. Cardiovasc Pathol. 2002; 11:135–140. [PubMed: 12031763]

Lee TY, Gotlieb AI. Microfilaments and microtubules maintain endothelial integrity. Microsc Res Tech. 2003; 60:115–127. [PubMed: 12500268]

Leonard SS, Castranova V, Chen BT, Schwegler-Berry D, Hoover M, Piacitelli C, Gaughan DM. Particle size-dependent radical generation from wildland fire smoke. Toxicology. 2007; 236:103–113. [PubMed: 17482744]

Leonard SS, Harris GK, Shi X. Metal-induced oxidative stress and signal transduction. Free Radic Biol Med. 2004; 37:1921–1942. [PubMed: 15544913]

Lin CY, Chen PC, Lin YC, Lin LY. Association among serum perfluoroalkyl chemicals, glucose homeostasis, and metabolic syndrome in adolescents and adults. Diabetes Care. 2009a; 32:702–707. [PubMed: 19114613]

Lin CY, Lin LY, Chiang CK, Wang WJ, Su YN, Hung KY, Chen PC. Investigation of the Associations Between Low-Dose Serum Perfluorinated Chemicals and Liver Enzymes in US Adults. Am J Gastroenterol. 2009b

Luebker DJ, Hansen KJ, Bass NM, Butenhoff JL, Seacat AM. Interactions of fluorochemicals with rat liver fatty acid-binding protein. Toxicology. 2002; 176:175–185. [PubMed: 12093614]

Lum H, Roebuck KA. Oxidant stress and endothelial cell dysfunction. Am J Physiol Cell Physiol. 2001; 280:C719–C741. [PubMed: 11245588]

Mehta D, Malik AB. Signaling mechanisms regulating endothelial permeability. Physiol Rev. 2006; 86:279–367. [PubMed: 16371600]

Nakagawa T, Hu H, Zharikov S, Tuttle KR, Short RA, Glushakova O, Ouyang X, Feig DI, Block ER, Herrera-Acosta J, Patel JM, Johnson RJ. A causal role for uric acid in fructose-induced metabolic syndrome. Am J Physiol Renal Physiol. 2006; 290:F625–F631. [PubMed: 16234313]

Nakayama K, Iwata H, Tao L, Kannan K, Imoto M, Kim EY, Tashiro K, Tanabe S. Potential effects of perfluorinated compounds in common cormorants from Lake Biwa, Japan: an implication from the hepatic gene expression profiles by microarray. Environ Toxicol Chem. 2008; 27:2378–2386. [PubMed: 18611081]

Nelson, JW.; Hatch, EE.; Webster, TF. Exposure to polyfluoroalkyl chemicals and cholesterol, body weight, and insulin resistance in the general U.S. population. Environ Health Persp. available at http://dx.doi.org/). Referenced 1-15-2010

Norman M. Low birth weight and the developing vascular tree: a systematic review. Acta Paediatr. 2008; 97:1165–1172. [PubMed: 18554273]

Oakes KD, Sibley PK, Martin JW, MacLean DD, Solomon KR, Mabury SA, Van Der Kraak GJ. Short-term exposures of fish to perfluorooctane sulfonate: acute effects on fatty acyl-coa oxidase activity, oxidative stress, and circulating sex steroids. Environ Toxicol Chem. 2005; 24:1172–1181. [PubMed: 16110997]

Olsen GW, Burris JM, Burlew MM, Mandel JH. Epidemiologic assessment of worker serum perfluorooctanesulfonate (PFOS) and perfluorooctanoate (PFOA) concentrations and medical surveillance examinations. J Occup Environ Med. 2003a; 45:260–270. [PubMed: 12661183]

Olsen GW, Burris JM, Ehresman DJ, Froehlich JW, Seacat AM, Butenhoff JL, Zobel LR. Half-life of serum elimination of perfluorooctanesulfonate, perfluorohexanesulfonate, and perfluorooctanoate in retired fluorochemical production workers. Environ Health Persp. 2007; 115:1298–1305.

Olsen GW, Gilliland FD, Burlew MM, Burris JM, Mandel JS, Mandel JH. An epidemiologic investigation of reproductive hormones in men with occupational exposure to perfluorooctanoic acid. J Occup Environ Med. 1998; 40:614–622. [PubMed: 9675720]

Olsen GW, Logan PW, Hansen KJ, Simpson CA, Burris JM, Burlew MM, Vorarath PP, Venkateswarlu P, Schumpert JC, Mandel JH. An occupational exposure assessment of a perfluorooctanesulfonyl fluoride production site: biomonitoring. Am Ind Hyg Assoc. 2003b; 64:651–659.

Parsons JR, Saez M, Dolfing J, de Voogt P. Biodegradation of perfluorinated compounds. Rev Environ Contam Toxicol. 2008; 196:53–71. [PubMed: 19025092]

Pelley J. Canada moves to eliminate PFOS stain repellents. Environ Sci Technol. 2004; 38:452A.

Qian Y, Baisden JM, Cherezova L, Summy JM, Guappone-Koay A, Shi X, Mast T, Pustula J, Zot HG, Mazloum N, Lee MY, Flynn DC. PC phosphorylation increases the ability of AFAP-110 to cross-link actin filaments. Mol Biol Cell. 2002; 13:2311–2322. [PubMed: 12134071]

Qian Y, Castranova V, Shi X. New perspectives in arsenic-induced cell signal transduction. J Inorg Biochem. 2003a; 96:271–278. [PubMed: 12888263]

Qian Y, Jiang BH, Flynn DC, Leonard SS, Wang S, Zhang Z, Ye J, Chen F, Wang L, Shi X. Cr (VI) increases tyrosine phosphorylation through reactive oxygen species-mediated reactions. Mol Cell Biochem. 2001; 222:199–204. [PubMed: 11678602]

Qian Y, Liu KJ, Chen Y, Flynn DC, Castranova V, Shi X. Cdc42 regulates arsenic-induced NADPH oxidase activation and cell migration through actin filament reorganization. J Biol Chem. 2005; 280:3875–3884. [PubMed: 15492012]

Qian Y, Luo J, Leonard SS, Harris GK, Millecchia L, Flynn DC, Shi X. Hydrogen peroxide formation and actin filament reorganization by Cdc42 are essential for ethanol-induced in vitro angiogenesis. J Biol Chem. 2003b; 278:16189–16197. [PubMed: 12598535]

Rosen MB, Schmid JE, Das KP, Wood CR, Zehr RD, Lau C. Gene expression profiling in the liver and lung of perfluorooctane sulfonate-exposed mouse fetuses: comparison to changes induced by exposure to perfluorooctanoic acid. Reprod Toxicol. 2009; 27:278–288. [PubMed: 19429403]

Schmidt A, Hall MN. Signaling to the actin cytoskeleton. Annu Rev Cell Dev Biol. 1998; 14:305–338. [PubMed: 9891786]

Seacat AM, Thomford PJ, Hansen KJ, Olsen GW, Case MT, Butenhoff JL. Subchronic toxicity studies on perfluorooctanesulfonate potassium salt in cynomolgus monkeys. Toxicol Sci. 2002; 68:249–264. [PubMed: 12075127]

Shao R, Guo X. Human microvascular endothelial cells immortalized with human telomerase catalytic protein: a model for the study of in vitro angiogenesis. Biochem Biophys Res Commun. 2004; 321:788–794. [PubMed: 15358096]

Shasby DM, Lind SE, Shasby SS, Goldsmith JC, Hunninghake GW. Reversible oxidant-induced increases in albumin transfer across cultured endothelium: alterations in cell shape and calcium homeostasis. Blood. 1985; 65:605–614. [PubMed: 3838256]

Siflinger-Birnboim A, Lum H, Del Vecchio PJ, Malik AB. Involvement of Ca2+ in the H2O2-induced increase in endothelial permeability. Am J Physiol. 1996; 270:L973–L978. [PubMed: 8764222]

Slotkin TA, MacKillop EA, Melnick RL, Thayer KA, Seidler FJ. Developmental neurotoxicity of perfluorinated chemicals modeled in vitro. Environ Health Persp. 2008; 116:716–722.

Steenland K, Tinker S, Frisbee S, Ducatman A, Vaccarino V. Association of perfluorooctanoic acid and perfluorooctane sulfonate with serum lipids among adults living near a chemical plant. Am J Epidemiol. 2009; 170:1268–1278. [PubMed: 19846564]

Stein CR, Savitz DA, Dougan M. Serum levels of perfluorooctanoic acid and perfluorooctane sulfonate and pregnancy outcome. Am J Epidemiol. 2009; 170:837–846. [PubMed: 19692329]

Taniyasu S, Kannan K, Horii Y, Hanari N, Yamashita N. A survey of perfluorooctane sulfonate and related perfluorinated organic compounds in water, fish, birds, and humans from Japan. Environ Sci Technol. 2003; 37:2634–2639. [PubMed: 12854699]

Vyalov S, Langille BL, Gotlieb AI. Decreased blood flow rate disrupts endothelial repair in vivo. Am J Pathol. 1996; 149:2107–2118. [PubMed: 8952543]

Washino N, Saijo Y, Sasaki S, Kato S, Ban S, Konishi K, Ito R, Nakata A, Iwasaki Y, Saito K, Nakazawa H, Kishi R. Correlations between prenatal exposure to perfluorinated chemicals and reduced fetal growth. Environ Health Persp. 2009; 117:660–667.

Wei Y, Shi X, Zhang H, Wang J, Zhou B, Dai J. Combined effects of polyfluorinated and perfluorinated compounds on primary cultured hepatocytes from rare minnow (Gobiocypris rarus) using toxicogenomic analysis. Aquat Toxicol. 2009; 95:27–36. [PubMed: 19712982]

Zhang X, Chen L, Fei XC, Ma YS, Gao HW. Binding of PFOS to serum albumin and DNA: insight into the molecular toxicity of perfluorochemicals. BMC Mol Biol. 2009; 10:16. [PubMed: 19239717]

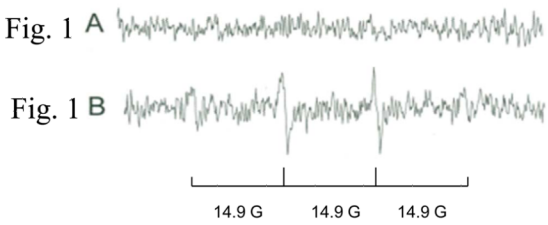

A – DMPO (100 mM) + Cells ($1x10^6$) PBS, 5 min 37°C
B - A + PFOS (100 .M)

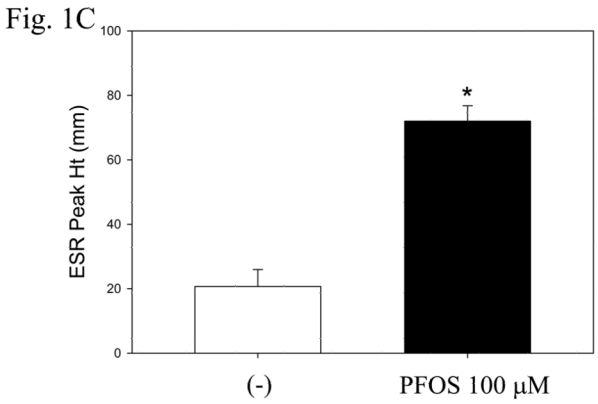

Figure 1. PFOS induces ROS generation in macrophages

ESR spectra were recorded 5 min after mixing 1×10^6 RAW 264.7 macrophages with 100 μM PFOS. The left panels are the ESR spectra, i.e., control (A) and cell exposed to PFOS (B). The right panel (C) represents quantification of ROS generation determined from analysis of signal peaks (n =4; * significant increase from control. $p < 0.05$).

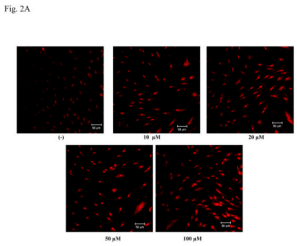

Fig. 2B

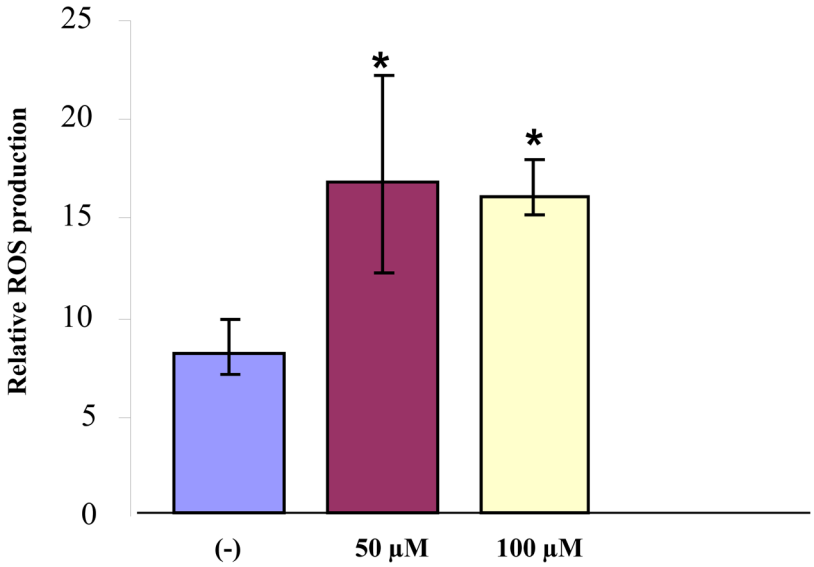

Figure 2. PFOS induces ROS generation in high range concentrations in HMVEC

A. HMVEC were grown on coverslips and serum-starved overnight. The cells were stimulated with different concentrations (10–100 μM) of PFOS for one hr. Dihydroethidium (DHE) dye was added into the cell culture during the last 30 min of the stimulation. After the staining, the cells were fixed and analyzed by confocal microscopy. The intensity of red color corresponds to the amount of ROS production. B. HMVEC were grown on 24-well plates and serum-starved overnight. The cells were stimulated with 50 μM and 100 μM PFOS, respectively, for 1 hr. Dihydroethidium dye was added into the cell culture during the last 30 min of the stimulation. After the staining, fluorescence was quantified with a microplate reader (n=3). * Statistically significantly different from control ($p<0.05$).

Fig. 3A

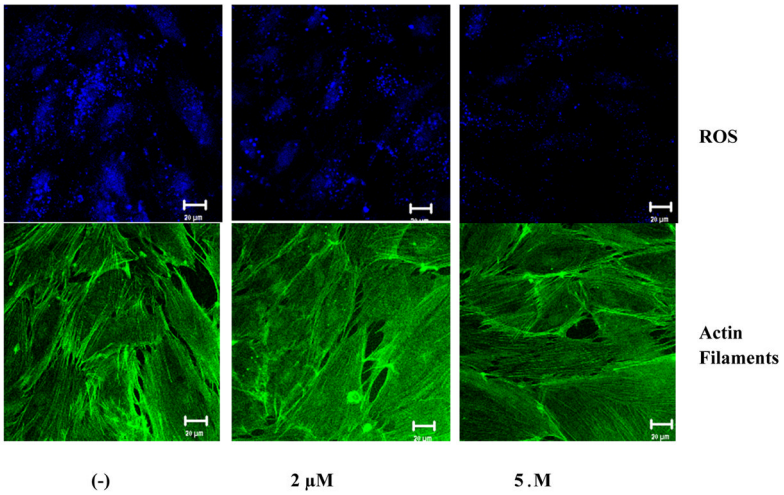

Fig. 3B

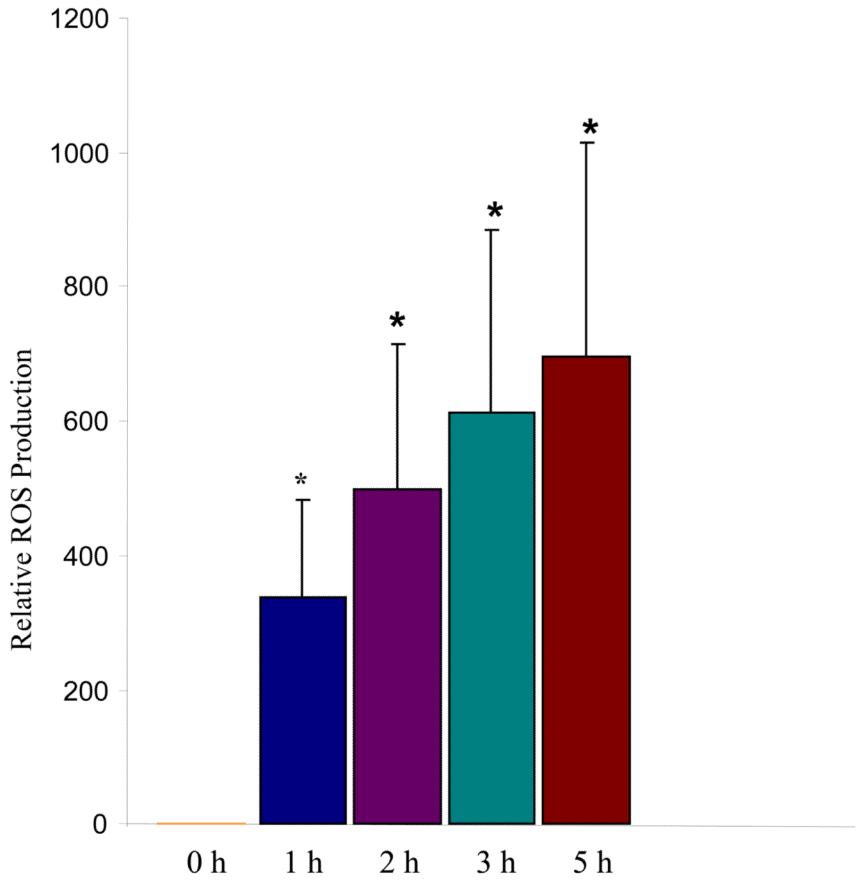

Figure 3. PFOS induces ROS generation in low range concentrations in HMVEC

A. HMVEC were grown on coverslips and serum-starved overnight. The cells were stimulated with the different concentrations (2 or 5 μM) of PFOS for 1 hr. Dihydroethidium dye was added into the cell culture during the last 30 min of the stimulation. After the staining, the cells were fixed and analyzed by confocal microscopy. The intensity of blue color inversely corresponds to the amount of ROS production (upper panels). The low panels are actin filament staining to reflect the cell number. B. PFOS induces ROS generation in a time-dependent manner in HMVEC. HMVEC were grown on 24-well plates and serum-starved overnight. The cells were stimulated with 2 μM of PFOS for the different periods of time (1–5 hrs) as indicated. Dihydroethidium dye was added into the cell culture during the last 30 min of the stimulation. After the staining, fluorescence was quantified with a microplate reader (n=4). * Significantly different from control ($p<0.05$).

Fig. 4A

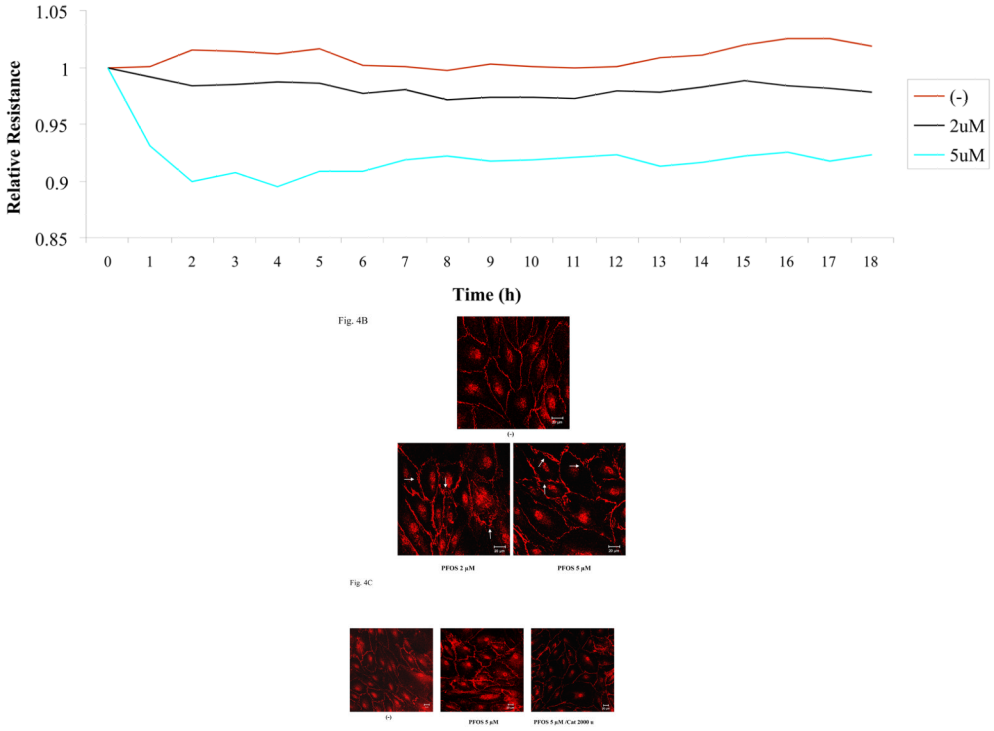

Figure 4. PFOS exposure induces an increase in HMVEC monolayer permeability through ROS production

A. HMVEC were grown to a confluent monolayer on gold microelectrodes and serum-starved overnight. The cells were exposed to different concentrations (2 or 5 μM) of PFOS as indicated, and measurements of the transendothelial resistance (TER) were performed using ECIS. The results shown are representative of 2 independent experiments. B. HMVEC were grown to a confluent monolayer on coverslides and serum-starved overnight. The cells were exposed to the different concentrations (2 or 5 μM) of PFOS as indicated for 1 hr. After the exposures, the cells were fixed, permeabilized, and stained with VE-cadherin (red color). A Zeiss confocal microscope was used to take the images. Arrows indicate the location of gaps. C. PFOS induces permeability through ROS production in HMVEC. HMVEC were grown to a confluent monolayer on coverslides and serum-starved overnight. The cells were exposed to PFOS (5μM), as well as catalase (2,000 u/ml), as indicated for 1 hr. After the exposures, the cells were fixed, permeabilized, and stained with VE-cadherin (red color). A Zeiss confocal microscope was used to take the images.

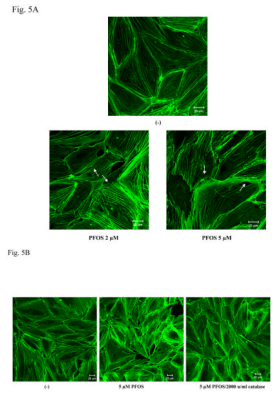

Fig. 5C

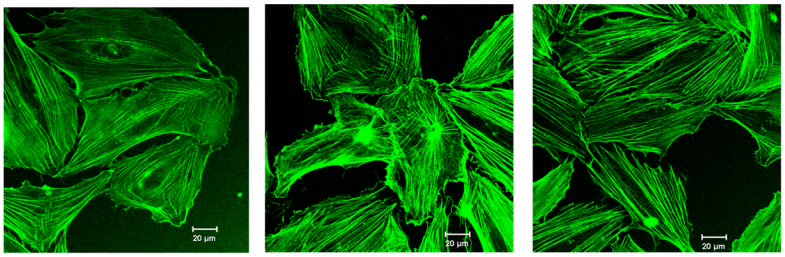

Figure 5. PFOS induces actin filament remodeling through ROS production in HMVEC

A. PFOS induces actin filament remodeling in confluent HMVEC monolayers. Confluent HMVEC on coverslips were serum-starved overnight and then were exposed to PFOS (2 or 5 μM) for 1 hr. After exposure, the cells were fixed, permeabilized, and stained with FITC-phalloidin to visualize actin filaments, followed by confocal microscopy analysis. Arrows indicate the disruption of DPB and the formation of break in the monolayers. B. PFOS induces actin filament remodeling through ROS production in confluent HMVEC monolayers. Confluent HMVEC on coverslips were serum-starved overnight and then were exposed to PFOS (5 μM), as well as catalase (2,000 u/ml), as indicated for 1 hr. After exposure, the cells were fixed, permeabilized, and stained with FITC-phalloidin for actin filaments, followed by confocal microscopy analysis as stated in Figure 5A. C. PFOS induces actin filament remodeling through ROS production in subconfluent HMVEC. HMVEC on coverslips were serum-starved overnight and then were exposed to PFOS (2 μM), as well as catalase (2,000 u/ml), as indicated for 1 hr. After the exposure, the cells were fixed, permeabilized, and stained FITC-phalloidin for actin filaments, followed by confocal microscopy analysis as stated in Figure 5A.

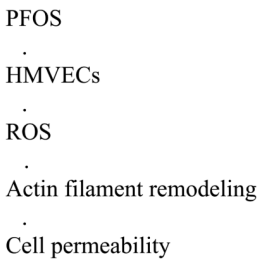

Figure 6. Schematic representation of signal transduction from PFOS stimulation to cell permeability